Vol. 38 (2007) ACTA PHYSICA POLONICA B No 2

TECHNICOLOUR AND OTHER BEYOND THE STANDARD MODEL ALTERNATIVES IN CMS*

Peter Kreuzer

University of Athens, Department of Physics, 157 84 Athens, Greece

(Received November 15, 2006)

The expected signal sensitivity of the $\rho_{\rm TC} \to W + Z \to 3\ell + \nu$ decay channel is studied for the CMS detector, under the Technicolour "Straw Man" model. It shows a signal discovery potential at integrated luminosities starting from $\int L dt \simeq 4\,{\rm fb}^{-1}$. Secondly, the CMS discovery potential of the heavy Majorana neutrino N_e and the right-handed gauge boson $W_{\rm R}$ is demonstrated, under the minimal LR symmetric model, at an early stage of the low luminosity running.

PACS numbers: 12.60.Nz, 12.90.+b

1. Search for Technicolour in the $\rho_{\rm TC} \to W + Z$ channel

Technicolour (TC) stands as an alternative to the elementary Higgs mechanism of the Standard Model (SM) and elegantly solves the naturalness, hierarchy and triviality problems [1, 2]. It introduces a new strong interaction with $(N_{\rm TC}^2 - 1)$ technigluons, at an energy scale $\Lambda_{\rm TC} \sim \nu_{\rm weak} \sim$ 200 GeV, providing a dynamical nature to Electroweak Symmetry Breaking (EWSB). The original model was developed and scaled from QCD, in particular the non-zero vacuum expectation value of a technifermion condensate, yielding technipions[1]. Technicolour spontaneously breaks electroweak interactions down to electromagnetism and the technipions (Goldstone bosons) become the longitudinal components of the SM gauge bosons W^{+-} and Z. The latter acquire their known masses, proportional to the technipion decay constant $F_\pi = 246\,{\rm GeV}$. As a consequence, the arbitrary introduction of any Higgs doublet is avoided in dynamic EWSB.

"Extended technicolour" (ETC) interactions must be introduced to produce the SM fermion masses: they are embedded in a larger gauge group ${\rm SU}(N_{\rm TC})\otimes$ ${\rm SU}(3)_{\rm C}\otimes{\rm SU}(2)_{\rm L}\otimes{\rm U}(1)_{\rm Y}$ and are broken down to colour and

* Presented at the "Physics at LHC" Conference, Kraków, Poland, July 3–8, 2006.

[1] Similarly to QCD, where a quark condensate yields pions at $\Lambda_{\rm QCD} \sim 200$ MeV.

technicolour at an energy scale $\Lambda_{\rm ETC} = M_{\rm ETC}/g_{\rm ETC}$. ETC interactions generate the masses of SM quarks and of any light technipion. Moreover, they give rise to quark mixing: experimental limits on Flavor Changing Neutral Currents (FCNC) force the scale $\Lambda_{\rm ETC}$ to lay around 100–1000 TeV. To obtain quark masses that are large enough then requires an enhancement of the technifermion condensate over that obtained by naive scaling from QCD. This occurs if the technicolour gauge coupling runs very slowly or "walks". Many technifermions N_D are typically needed in "Walking TC" [1], reducing the expected energy scale (< 1 TeV) of the lightest technicolour resonances technirho ($\rho_{\rm TC}$) and techniomega ($\omega_{\rm TC}$). The model is completed with topcolour-assisted technicolour (TC2) [3], in order to integrate the generation of the top quark mass.

The present analysis [4] is performed under the phenomenology of the lowest-lying technihadrons, commonly referenced as the technicolour "Straw Man" model (TCSM) [5]. The colour-singlet sector includes the pseudoscalar technimesons $\pi_{\rm TC}$ and the vector technimesons $\rho_{\rm TC}$ and $\omega_{\rm TC}$. The decay of $\rho_{\rm TC}$ is expressed as an admixture of $\pi_{\rm TC}$ and the Standard Model Z and W bosons:

$$\rho_{\rm TC} \rightarrow \cos^2\chi \langle \pi_{\rm TC}\pi_{\rm TC}\rangle + 2\cos\chi\sin\chi \langle \pi_{\rm TC} W_{\rm L}\rangle + \sin^2\chi \langle W_{\rm L} W_{\rm L}\rangle\,, \tag{1.1}$$

where $W_{\rm L}$ is the longitudinal mode of the Z or W and $\sin\chi \simeq 1/\sqrt{N_D} \sim 1/3$. The branching fraction BR($\rho_{\rm TC} \rightarrow W + Z$) is competing with the two first terms in (1), hence with $M(\pi_{\rm TC})$.

From the experimental point of view, the basic element is the search for a resonance decaying into dibosons. In particular, the decay channel $\rho_{\rm TC} \rightarrow W + Z$ has the advantage of a very clean final state, namely $3\ell + \nu$; the corresponding production diagram is shown in Fig. 1.

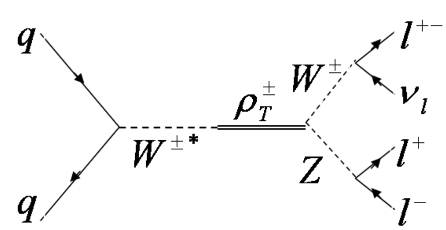

Fig. 1. Main $\rho_{\rm TC} \rightarrow W + Z$ production mode at LHC.

Other decay modes including jets, like $\rho_{\rm TC} \rightarrow W + \pi_{\rm TC} \rightarrow \ell\,\nu\, b\bar{b}$, have better branching fractions but are more difficult to disentangle from the Standard Model processes. The most relevant background contributions to the signal in Fig. 1 are $WZ \rightarrow 3\ell + \nu$ (labeled "WZ" below), $ZZ \rightarrow 4\ell$ (labeled "ZZ" below), $Zb\bar{b} \rightarrow 2\ell + X$ (labeled "$Zb\bar{b}$" below) and $t\bar{t}$.

1.1. Event reconstruction and selection path

All signal and background samples used in this analysis are generated with PYTHIA 6.2 [6][2] with the requirement of at least 3 prompt leptons in the CMS fiducial region. A set of 14 different $\rho_{\rm TC}$ samples are generated within the $[{\rm M}(\rho_{\rm TC}), {\rm M}(\pi_{\rm TC})]$ phase space.

The CMS fast simulation (FAMOS_1_4_0 [8]) is used for detector simulation and event reconstruction. Event pileup is taken into account, according to the low instantaneous luminosity scenario of $2 \times 10^{33}{\rm cm}^{-2}{\rm s}^{-1}$, and nominal CMS Level-1 and High-Level Trigger (HLT) requirements are applied [9]. The main reconstructed objects are leptons (muons and electrons) and the Missing Transverse Energy; their reconstruction quality and efficiency have been validated against the detailed GEANT-based CMS detector simulation [10]. The analysis path is summarized as follows:

(i) Lepton Selection: 3 high-$p_{\rm T}$ and isolated electrons or muons.

(ii) Lepton Trigger: single- or two-electron or muon mode.

(iii) Z: same-flavor/opp.-charge ℓ-pair closest to $M(Z)$, $p_{\rm T} > (30{,}10){\rm GeV}/c$.

(iv) W: 3rd lepton with $p_{\rm T} > 10\,{\rm GeV}/c$ + Missing $E_{\rm T}$ + $M(W)$ constraint.

(v) $|\,{\rm M}(\ell^+\ell^-) - {\rm M}(Z)\,| \leq 3\sigma_{{\rm M}_Z} \cong 7.8\,{\rm GeV}/c^2$.

(vi) $p_{\rm T}(Z)$ and $p_{\rm T}(W) > 30\,{\rm GeV}/c$[3].

(vii) $|\Delta[\eta(Z) - \eta(W)]| \leq 1.2$.

The Z and W are reconstructed with a purity of $\sim$99%, using the 3 highest-$p_{\rm T}$ leptons in the event. The Missing $E_{\rm T}$ is obtained as the vector sum of the jets in the event ("Iterative Cone" algorithm), with an energy resolution of 23% for signal events. The $M(W)$ constraint yields a 2 fold ambiguity in the p_Z component of the reconstructed neutrino: it is found that the most efficient choice for the $\rho_{\rm TC}$ signal is the minimum p_Z solution. The kinematic cuts are illustrated in Fig. 2. The main $t\bar{t}$ reduction is obtained via the Z-mass window requirement *(v)*. The irreducible background $WZ \to 3\ell + \nu$ is most efficiently separated from the signal via the $\eta(Z) - \eta(W)$ correlation requirement *(vii)*. The $p_{\rm T}$ cut on Z and W further improves the signal to background ratio, however, it is kept modest in order to preserve the exponential background hypothesis of the $3\ell + \nu$ invariant mass spectrum, used to compute the signal sensitivity. The $\rho_{\rm TC}(300)$ signal and background yields are shown in Fig. 2(d) and the corresponding reconstruction efficiencies are listed in Table I.

---

[2] The $Zb\bar{b}$ background is generated using CompHEP [7] interfaced to PYTHIA.

[3] For benchmark points with $M(\rho_{\rm TC}) = 200\,{\rm GeV}/c^2$, the minimum $p_{\rm T}(Z)$ and $p_{\rm T}(W)$ threshold is $10\,{\rm GeV}/c$.

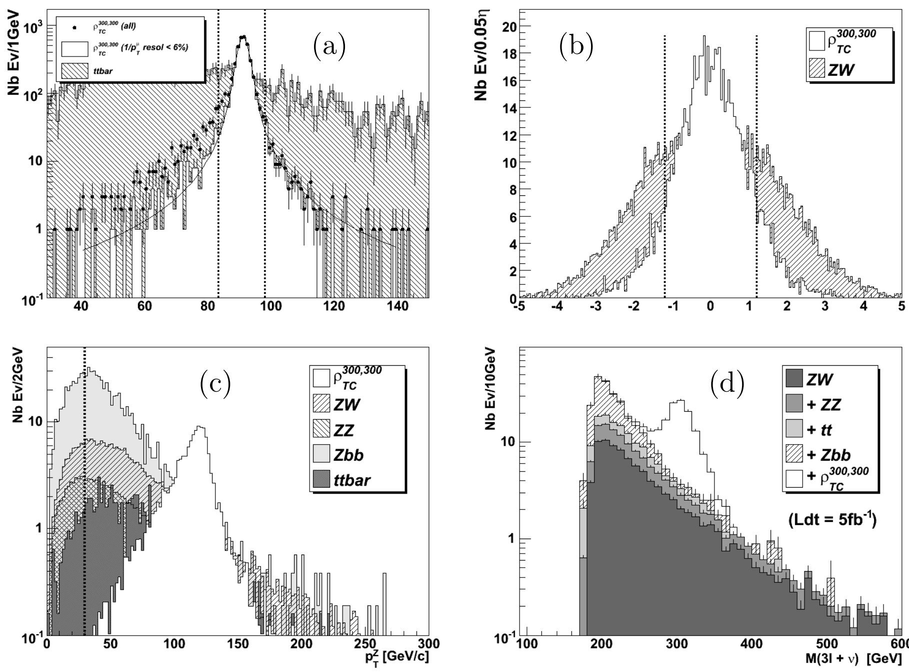

Fig. 2. (a) $M(\mu^+\mu^-)$ for $\rho_{\rm TC}(300)$ and $t\bar{t}$; (b) $\Delta[\eta(Z)-\eta(W)]$ for $\rho_{\rm TC}(300)$ and WZ; (c) $p_{\rm T}(Z)$ for $\rho_{\rm TC}(300)$ and all backgrounds ($p_{\rm T}(W)$ is similar); (d) Reconstructed $(M3\ell+\nu)$ for $\rho_{\rm TC}(300)$ and all backgrounds. The vertical lines indicate the applied requirements.

TABLE I

$\sigma\,\times\,{\rm BR}\,(\ell=\,e\,{\rm or}\,\mu)$, 3-lepton preselection efficiency, total efficiency and final yield within 3σ of the signal region ($N_{\rm event}$), for $\mathcal{L}=5{\rm fb}^{-1}$. $\rho_{\rm TC}(300)$ and the main background contributions are shown. The simulation is repeated for all $\rho_{\rm TC}$ benchmark points.

Sample	$\sigma\times{\rm BR}$(pb)	ε(3-lept)	ε(Reco) (%)	$N_{\rm event}\,(5{\rm fb}^{-1})$
$\rho_{\rm TC}\to W+Z$	0.13	0.635	25.88 ± 0.40	103
$WZ\to 3\ell+\nu$	0.39	0.471	9.91 ± 0.11	27
$ZZ\to 4\ell$	0.07	0.719	15.80 ± 0.14	10
$Zb\bar{b}\to 2\ell+X$	332	0.046	0.23 ± 0.01	12
$t\bar{t}$	489.72	0.065	0.019 ± 0.001	8

1.2. Signal sensitivity and systematic uncertainties

The sensitivity of each $\rho_{\rm TC}$ benchmark point is computed by taking into account realistic statistical fluctuations for a given integrated luminosity. The sensitivity estimator is defined as the likelihood-ratio $S_{\rm L} = \sqrt{2\ln(\mathcal{L}_{\rm S+B}/\mathcal{L}_{\rm B})}$, where $\mathcal{L}_{\rm S+B}$ and $\mathcal{L}_{\rm B}$ are the best-fit likelihoods of the signal-plus-background hypothesis and the null hypothesis (no signal present). The signal probability density function (p.d.f.) is assumed Gaussian (dominated by detector resolution) and the background p.d.f. is exponential in all $\rho_{\rm TC}$ fit regions. The output of the fitting procedure is shown in the contour plot over the $[{\rm M}(\rho_{\rm TC}), {\rm M}(\pi_{\rm TC})]$ phase space in Fig. 3 (left), for various integrated luminosities. A signal sensitivity above 5 is expected for $\mathcal{L} = 3\,{\rm fb}^{-1}$ (before including systematic uncertainties).

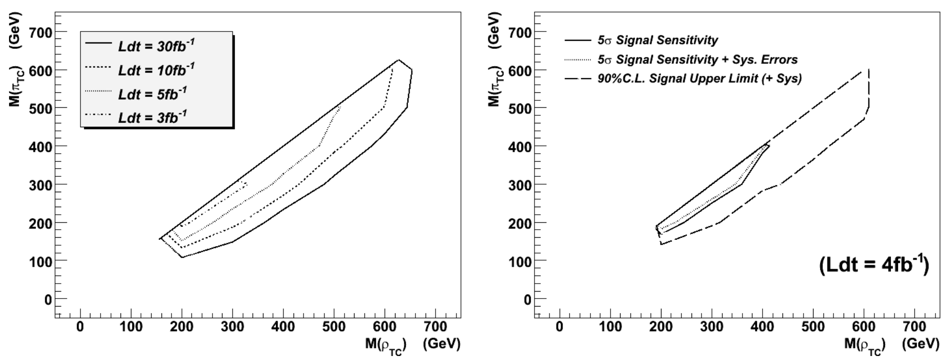

Fig. 3. Signal 5σ sensitivity curves for various integrated luminosities (left); sensitivity for $\mathcal{L} = 4\,{\rm fb}^{-1}$: the dotted (dashed, respectively) curve shows the sensitivity (the 90% C.L. signal upper limit, respectively) after including systematic uncertainties (right).

The $\rho_{\rm TC}$ sensitivity has been simulated for the early CMS data taking phase. Expected detector related systematic uncertainties for $\mathcal{L} = 1{\rm fb}^{-1}$ are taken into account. While no substantial contribution is found from the tracker and muon system misalignment or the calorimeter miscalibration, the accuracy at which the lepton efficiency will be determined from data affects the result: a 2% uncertainty is considered. Moreover, the lepton fake rate has been simulated on $Zb\bar{b}$ and extrapolated to any Z+jet(s) type background[4], in order to take into account additional contaminations from pion/kaon decays or from wrongly identified lepton candidates: a single lepton fake rate of $O(10^{-3})$ is obtained with FAMOS, affecting the $\rho_{\rm TC}$ sensitivity as shown below. Finally, a 7.5% uncertainty on the missing $E_{\rm T}$ (MET) measurement is considered. The above uncertainties result in

[4] A production cross-section of 1047 pb per lepton flavor is assumed for $Z + n$-jets.

the relative ρ_{TC} sensitivity drop $\Delta^{\mathrm{tot}}_{\mathrm{SYS}} = \sqrt{(\Delta_{\mathrm{Eff}})^2 + (\Delta_{\mathrm{Fake}})^2 + (\Delta_{\mathrm{MET}})^2}$ $= \sqrt{(2.7\%)^2 + (8.5\%)^2 + (6.6\%)^2} = 11\%$. Concerning the generated cross section, introducing Next-to-Leading-Order K-factors for signal and background leads to a relative signal sensitivity increase of 6%; however the latter correction is not included in the final result shown in Fig. 3 (right).

2. Detection of heavy Majorana neutrinos and right-handed bosons

Left–right (LR) symmetric models represent another interesting extension of the Standard Model, since they naturally explain parity violation of electroweak interactions. In particular, the minimal LR symmetric model [11, 12] built under the gauge symmetry group $\mathrm{SU_C}(3)\otimes\mathrm{SU_L}(2)\otimes\mathrm{SU_R}(2) \otimes \mathrm{U}(1)$ embeds the SM at the scale of the order 1 TeV and the Higgs sector consists of a bi-doublet and two triplets. Three additional gauge bosons W_{R} and Z' necessarily appear, together with the heavy Majorana neutrino states (N_ℓ) [13]. The latter can provide non-zero masses to their lighter partners ν_ℓ via the see-saw mechanism [14]. The relevance of LR symmetric models has increased since the experimental evidence of neutrino oscillations [15]. Existing experimental data have set lower bounds to the Z' and W_{R} masses of O(1) TeV [16] and 1.6 TeV [17], respectively, with large uncertainties. This analysis [18] is performed under the assumption $M(W_{\mathrm{R}}) > 1$ TeV.

Among several production modes of N_ℓ and W_{R} in pp collisions, the most promising in terms of cross-section and the most suitable for heavy neutrino searches is given in Fig. 4. At LHC energies, the electron flavor N_e is expected to dominate heavier flavors, yielding the signature $pp \to e + N_e \to e + eW_{\mathrm{R}} \to 2e + 2\,\mathrm{jets}$.

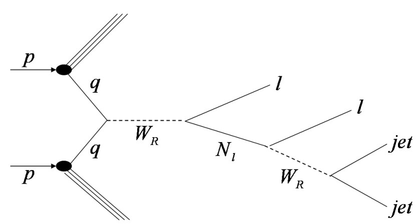

Fig. 4. Heavy Majorana neutrino N_ℓ production through a W_{R} boson.

The main background contributions are expected from SM processes with a lepton pair and at least two jets in the final state, namely WZ (leptonic W decays only and no hadronic Z decays), Z+ jets, $t\bar{t}$ (leptonic W decays only), ZH and WH.

2.1. Event reconstruction and selection path

All signal and background events are generated and their cross section computed with PYTHIA 6.2 [6]. The signal uses default CTEQ5L parton distribution functions [19] and the set of parameters listed in [18].

The reconstruction is performed with the GEANT-based full CMS detector simulation [10]. Event pileup is taken into account, according to the low instantaneous luminosity scenario of $2 \times 10^{33}\mathrm{cm}^{-2}\mathrm{s}^{-1}$, and nominal Level-1 (HLT respectively) electron trigger requirements [9] are applied, yielding a signal efficiency of 100 % (99 % respectively). All reconstructed electron[5] candidates are required to satisfy $E_{\mathrm{T}} > 20\,\mathrm{GeV}$ and a Tracker isolation flag is set within a cone of radius 0.3 around the electron track. Jets are reconstructed by the Iterative Cone algorithm, with a minimum E_{T} requirement of 40 GeV.

A primary selection of at least 2 isolated electrons and 2 jets is made. Furthermore, only events with two isolated electrons are kept (e_1, e_2), with the invariant mass requirement $M_{e_1e_2} > 200\,\mathrm{GeV}$, and only the two highest-p_{T} jets are considered (j_1, j_2). A mass window of 110 GeV (optimized on S/B) is required around the reconstructed heavy neutrino invariant mass $M_{N_e}^{\mathrm{cand}} = M_{ej_1j_2}$[6] and a threshold of 1 TeV is required on the combined system $M_{W_{\mathrm{R}}}^{\mathrm{cand}} = M_{e_1e_2j_1j_2}$. The event yields throughout the selection path are shown in Table I, for the signal benchmark point $(M_{N_e},\ M_{W_{\mathrm{R}}}) = (500, 2000)$ GeV (called LRRP below) and for all significant background contributions.

TABLE II

Event yields throughout the selection path, for signal and background. Due to processing limitations, only a fraction of $Z+$jets events are fully simulated.

Step	Signal	$t\bar{t}$	$Z+$jets	ZW	WH
Generated	4965	2.64×10^6	6.2×10^7	6×10^4	11000
Primary selection	2782	1.5×10^5	—	38	728
2 isolated e	2332	152000	—	15	165
$M_{e_1e_2} > 200$ GeV	2246	17200	3870	0	72
$M_{N_e}^{\mathrm{cand}}$ window	970	3430	1000	0	2
$+ M_{W_{\mathrm{R}}}^{\mathrm{cand}} > 1$ TeV	938	198	96	0	0

[5] For simplicity, positrons are called "electrons" in the text.
[6] Both combinations $e_1j_1j_2$ and $e_2j_1j_2$ are kept in the final spectra.

The $Z+$jets background has the largest production cross section and is reduced by minimum E_{T} requirements on reconstructed electron and jet objects. The $M_{e_1e_2}$ cut dramatically improves the S/B ratio of any type of reaction including a Z. The largest background contribution after full selection is $t\bar{t}$. It has been checked that only leptonic W decay modes from $t\bar{t}$ contribute. Finally, backgrounds containing a Higgs are almost negligible, due to their relatively small production cross section.

The heavy Majorana neutrino search will be performed by first selecting events with $M_{W_{\mathrm{R}}}^{\mathrm{cand}} > 1\,\mathrm{TeV}$, followed by a scan over the reconstructed $M_{N_e}^{\mathrm{cand}}$ spectrum. This is illustrated in Fig. 5, for an integrated luminosity of $\int L dt = 30\,\mathrm{fb}^{-1}$: a large S/B ratio is expected for the LRRP benchmark point.

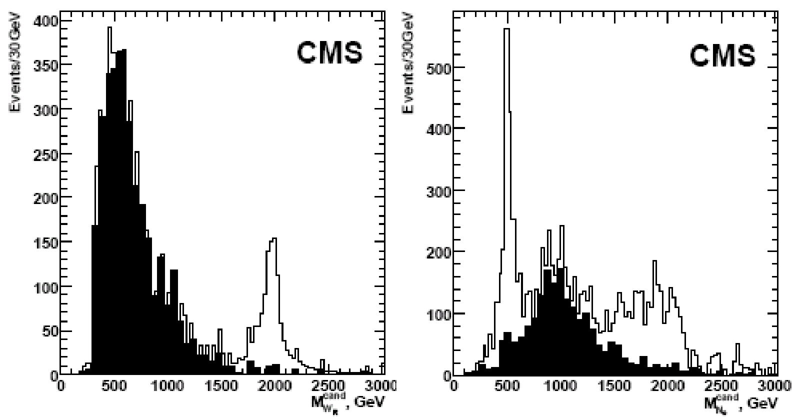

Fig. 5. Reconstructed gauge boson W_{R} invariant mass (left); reconstructed heavy Majorana neutrino N_e invariant mass, after a 1 TeV threshold has been required on $M_{W_{\mathrm{R}}}^{\mathrm{cand}}$ (right). The signal is shown in open white and the total background in shaded style.

2.2. Signal sensitivity and systematic uncertainties

The expected discovery potential of N_e and W_{R} at CMS is calculated using the significance estimator $S = 2(\sqrt{N_{\mathrm{S}} - N_{\mathrm{B}}} - \sqrt{N_{\mathrm{B}}}) \geq 5$ [20]. The corresponding discovery contours are shown in Fig. 6, for various integrated luminosities. Invariant mass regions up to $(M_{N_e}, M_{W_{\mathrm{R}}}) = (3.5, 2.3)\,\mathrm{TeV}$ are reachable after 3 years of running at low luminosity ($\int L dt = 30\,\mathrm{fb}^{-1}$). Lower mass regions (*e.g.* the LRRP benchmark point) are reachable after only a few fb^{-1}.

The expected uncertainty of this prediction related to various systematic background uncertainties is small, since the background itself is small. The discovery region is mainly limited by the fast drop of the signal cross section at high ratios $r = M_{N_e}/M_{W_{\rm R}}$ or by the fast drop of signal efficiency at small r, and the contours on Fig. 6 are barely affected by systematic uncertainties. As for the generated signal cross sections, various parton density functions sets have been used to take into account theoretical fluctuations [21]: they lead to a 6% uncertainty on the cross section and to a systematic error of 1–3 % on the significance prediction over whole discovery region.

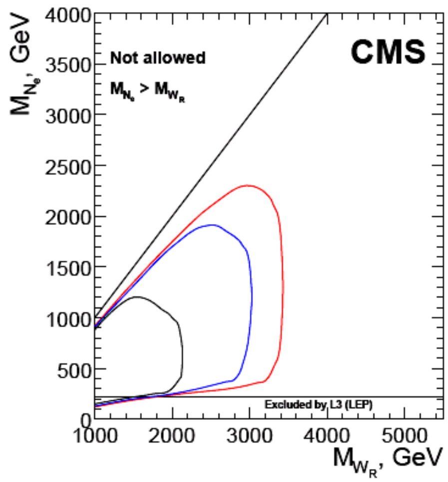

Fig. 6. CMS discovery potential of the heavy Majorana neutrino N_e and the right-handed gauge boson $W_{\rm R}$ for $\int Ldt = 30, 10$ and $1\,{\rm fb}^{-1}$ (from outer to inner coutour, respectively). The horizontal exclusion line was set by the L3 experiment [22].

3. Conclusions

The signature $\rho_{\rm TC} \to W + Z$ in the context of the Technicolour "Straw Man" model is studied for the CMS detector. A 5 sigma discovery reach is obtained for an integrated luminosity $\mathcal{L} \simeq 4\,{\rm fb}^{-1}$. The discovery potential of the heavy Majorana neutrino N_e and the right-handed gauge boson $W_{\rm R}$ is demonstrated, under the minimal LR symmetric model, for only a few ${\rm fb}^{-1}$ of running at CMS. Both predictions represent a potential handle into Physics Beyond the Standard Model, at an early stage of the LHC era.

REFERENCES

[1] K. Lane, `hep-ph/0007304`.
[2] K. Lane, `hep-ph/0202255`.
[3] C.T. Hill, *Phys. Lett.* **B345**, 483 (1995) [`hep-ph/9411426`].
[4] P. Kreuzer, CMS Note, **2006-135**, (2006).

[5] K. Lane, S. Mrenna, *Phys. Rev.* **D67**, 115011 (2003).
[6] T. Sjostrand, L. Lonnblad, S. Mrenna, `hep-ph/0108264`.
[7] A. Pukhov *et al.*, `hep-ph/9908288`.
[8] CMS Collaboration, CERN/LHCC, **2006-001**, CMS TDR 8.1 (2006).
[9] CMS Collaboration, CERN/LHCC, **2002-26**, CMS TDR 6.2, (2002).
[10] S. Wynhoff *et al.*, `http://cmsdoc.cern.ch/orca`.
[11] R.N. Mohapatra, J.C. Pati, *Phys. Rev.* **D11**, 2558 (1975).
[12] G. Senjanovic, R.N. Mohapatra, *Phys. Rev.* **D12**, 1502 (1975).
[13] M. Gell-Mann *et al.*, *Supergravity*, Proceedings of the workshop at Stony Brook, 27–29 September 1979, ed. North-Holland, Amsterdam 1979, p. 341.
[14] R.N. Mohapatra, G. Senjanovic, *Phys. Rev. Lett.* **44**, 912 (1980).
[15] C. Giunti, M. Laveder, `hep-ph/0310238`.
[16] (Particle Data Group) S. Eidelman *et al.*, *Phys. Lett.* **B592**, 1 (2004).
[17] G. Barenboim, J. Bernabeu, J. Prades, M. Raidal, *Phys. Rev.* **D55**, 4213 (1997).
[18] S.N. Gninenko, M.M. Kirsanov, N.V. Krasnikov, V.A. Matveev, CMS Note, **2006-098**, (2006).
[19] J. Botts *et al.*, *Phys. Lett.* **B304**, 159 (1993).
[20] S.I. Bityukov, N.V. Krasnikov, `hep-ph/0204326`.
[21] P. Bertalini, R. Chierci, A. De Roeck, CMS Note, **2005-013**, (2005).
[22] P. Achard *et al.*, (L3 Collaboration), *Phys. Lett.* **B517**, 67 (2001).